

# Effect of asiatic acid on epithelial-mesenchymal transition of human alveolar epithelium A549 cells induced by TGF- $\beta$ 1

QINGRONG CUI<sup>1\*</sup>, JUAN REN<sup>2\*</sup>, QINGWEI ZHOU<sup>1</sup>, QINMEI YANG<sup>1</sup> and BIN LI<sup>1</sup>

<sup>1</sup>Department of Respiration, The First Affiliated Hospital of Henan University of CM, Zhengzhou, Henan 450000;

<sup>2</sup>Department of Oncology, Hangzhou Third Hospital, Hangzhou, Zhejiang 310009, P.R. China

Received June 1, 2018; Accepted January 25, 2019

DOI: 10.3892/ol.2019.10140

**Abstract.** Asiatic acid (AA) is a pentacyclic triterpenoid isolated from *Centella asiatica* (L.) Urban that possesses significant antitumor activities. In the present study, the mechanism of AA on transforming growth factor- $\beta$ 1 (TGF- $\beta$ 1)-induced epithelial-mesenchymal transition (EMT) was investigated in the lung cancer cell line A549. To do so, cell morphological alterations were observed and recorded at different time periods. Cells treated with TGF- $\beta$ 1 were spindle-shaped and characterized as stromal cells, whereas AA-treated cells exhibited epithelial cell characteristics and increased intercellular adhesion. The MTT assay demonstrated that the high concentration of AA inhibited the viability of A549 cells treated with TGF- $\beta$ . In addition, the wound healing and Transwell assays revealed that AA inhibited TGF- $\beta$ 1-induced invasion and migration of A549 cells. Furthermore, AA treatment increased the mRNA and protein expression levels of E-cadherin, and decreased the expression levels of snail family transcriptional repressor (Snail), N-cadherin, vimentin and  $\beta$ -catenin in TGF- $\beta$ 1-treated A549 cells. In conclusion, these results suggested that AA may inhibit TGF- $\beta$ 1-induced EMT in lung cancer through increased expression of E-cadherin, and inhibition of Snail, N-cadherin and vimentin expression.

## Introduction

Lung cancer is the principal cause of cancer-associated mortality worldwide and is associated with high morbidity. Non-small cell lung cancer (NSCLC) accounts for 80-85%

of all lung cancer cases (1). According to a previous study, >234,030 new lung cancer cases are predicted to occur every year, and 154,050 cases of lung cancer-associated mortality are predicted in the USA (2). Furthermore, the World Health Organization predicts that 1,000,000 cases of lung cancer-associated mortality may be reached by 2025 in China (3). Although advances have been made in conventional cancer therapies, including diagnostic imaging, surgery, radiotherapy and chemotherapy, the 5-year survival rate of patients with NSCLC remains poor, mostly due to drug resistance and tumor metastasis (4). Metastasis is a sign of malignancy and a common characteristic of lung cancer, and is the major reason for treatment failure and patient mortality. Approximately 30% of patients present distant metastases at admission, 50-60% develop distant metastases during treatment and 80-90% succumb to metastases (5). Recently, specific targeted drugs have been developed for lung cancer treatment, including the epidermal growth factor receptor, and the tumor angiogenesis inhibitors gefitinib and bevacizumab (6). However, the high recurrence and metastasis rates seriously affect the quality of life and overall survival of patients (7). Understanding the molecular mechanisms underlying lung cancer may provide novel strategies for lung cancer treatment, and improve the survival rate and quality of life for patients with lung cancer; however, such advances remain largely elusive. Understanding such mechanisms may provide a foundation for the development of novel therapeutic approaches.

Asiatic acid (AA) is a pentacyclic triterpenoid extracted from the umbelliferous plant *Centella asiatica* (L.) Urban. Previous studies have demonstrated that AA serves a role in inhibiting lung cancer cell growth *in vitro* and *in vivo* through mitochondrial damage (8,9). In addition, it has been suggested that AA possesses pharmacological activities, including inhibition of cancer proliferation, apoptosis-inducing effects and anti-metastatic effects in various types of tumor (10-12). Previous studies have suggested that epithelial-mesenchymal transition (EMT) serves a crucial role in primary invasion and secondary metastasis of various types of cancer. EMT is characterized by reduced expression of the cell adhesion molecule E-cadherin, increased expression of the cytoskeletal component vimentin and enhanced mesenchymal cell morphology (13-15). Tumor metastasis results from molecular structure modifications that promote cell invasion and

---

*Correspondence to:* Professor Qingwei Zhou, Department of Respiration, The First Affiliated Hospital of Henan University of CM, 19 Renmin Road, Zhengzhou, Henan 450000, P.R. China  
E-mail: zhouqingwei2010@126.com

\*Contributed equally

*Abbreviations:* AA, asiatic acid; EMT, epithelial-mesenchymal transition; TGF- $\beta$ 1, transforming growth factor- $\beta$ 1

*Key words:* asiatic acid, EMT, invasion, lung cancer, migration

diffusion to other areas. Identification of factors regulating EMT would therefore be highly valuable for the treatment of tumor metastasis. EMT is controlled by various transcription factors, including transforming growth factor- $\beta$ 1 (TGF- $\beta$ 1). TGF- $\beta$ 1 is a member of the TGF- $\beta$  superfamily that contributes to EMT during embryonic development and induces EMT during tumor progression (16). AA has inhibitory effects on various types of tumor; however, to the best of our knowledge, its antitumor activity through EMT inhibition in cancer cells remains unknown (17,18).

In the present study, the human alveolar epithelium A549 cell line was used to study the anticancer effects and underlying mechanisms of AA. To do so, the TGF- $\beta$ 1-induced EMT model was used to explore the antitumor effects of AA on EMT and its efficacy against lung cancer.

## Materials and methods

**Cells and reagents.** The human A549 lung cancer cell line was purchased from the Cell Bank, Shanghai Institute of Life Science, Chinese Academy of Science (Shanghai, China). Cells were maintained in Roswell Park Memorial Institute (RPMI)-1640 culture medium (Gibco; Thermo Fisher Scientific, Inc., Waltham, MA, USA) supplemented with 10% fetal bovine serum (FBS; Gibco; Thermo Fisher Scientific, Inc.) and 100 U/ml penicillin/streptomycin (Sigma-Aldrich; Merck KGaA, Darmstadt, Germany), and were incubated at 37°C in a humidified atmosphere containing 5% CO<sub>2</sub>. Cells in the exponential growth phase (~80% confluence) were used in all experiments. AA was purchased from Sigma-Aldrich; Merck KGaA.

**Establishment of the EMT model of A549 cells.** The A549 cells were washed with PBS and cultured with 1 ml 0.25% trypsin. The trypsin was then removed and the cells were resuspended in complete medium. After complete digestion, cells in the logarithmic growth phase were harvested and seeded in 6-well plates at a density of 8x10<sup>5</sup> cells/well in 2 ml medium. Following overnight incubation, cells were divided into three groups, as follows: A negative control group, a TGF- $\beta$ 1-treated group (10 ng/ml) and an AA + TGF- $\beta$ 1-treated group (20  $\mu$ mol/l AA + 10 ng/ml TGF- $\beta$ 1). Each condition was set up in triplicate. Cells were treated for 24 h, after which, A549 cell morphology and growth were observed and images were captured under an inverted microscope (Leica Microsystems GmbH, Wetzlar, Germany).

**Cell viability assay.** Cell viability was measured using the colorimetric MTT assay as described previously (19). After complete digestion, cells in the logarithmic growth phase were harvested and seeded in 96-well plates at a density of 1x10<sup>4</sup> cells/well in 100  $\mu$ l medium, and incubated in serum-free medium for 24 h. Cells were then treated with increasing concentrations of AA (5, 10, 20, 40 and 80  $\mu$ mol/l) with or without TGF- $\beta$ 1 or medium for 24 h. MTT reagent (100  $\mu$ l, 1 mg/ml) was added to the cells for 4 h. Eventually, the supernatant was removed and the purple formazan crystals generated by viable cells were dissolved with 100  $\mu$ l dimethyl sulfoxide, prior to measuring absorbance at 570 nm with a microplate reader (Multiskan Spectrum; Molecular Devices, LLC, Sunnyvale, CA, USA).

**Wound healing assay.** A549 cell migration was assessed with the wound healing assay as previously described (20). Briefly, A549 cells were seeded in 12-well plates at a density of 1x10<sup>5</sup> cells/well in 1 ml medium and cultured in an incubator for 24 h. Subsequently, a horizontal wound was generated with a 10- $\mu$ l pipette tip, cells were washed with PBS to remove cell debris, and were incubated with culture medium (control) or TGF- $\beta$ 1 with or without AA (10, 20 or 40  $\mu$ mol/l) for 24 h. The migration status was observed under a fluorescence microscope at 0 and 24 h. The wound healing rate was used to evaluate cell migration ability and quantified as follows: (wound width at 0 h-wound width at 24 h)/wound width at 0 h with ImageJ V1.8.0 software (National Institutes of Health, MD, USA) (21). Experiments were performed three times.

**Transwell assay.** Cell migratory and invasive capacities were assessed with specialized Transwell chambers (8- $\mu$ m pores; BD Biosciences, San Jose, CA, USA). For the migration assay, 150  $\mu$ l cell suspension (1x10<sup>5</sup> cells/ml) containing the appropriate drugs [TGF- $\beta$ 1 (10 ng/ml) or AA + TGF- $\beta$ 1 (10, 20 or 40  $\mu$ mol/l AA + 10 ng/ml TGF- $\beta$ 1)] was added to the upper chamber of a Transwell system, and 450  $\mu$ l culture medium containing 15% FBS was added to the lower chamber. After 48 h incubation, any non-migrating or non-invading cells on the upper surface were removed. Cells in the lower chamber were fixed with 4% paraformaldehyde for 30 min at room temperature, and stained with the 0.1% crystal violet for 30 min at room temperature. The number of migrated cells was counted randomly under a light microscope (magnification, x200, three fields/well). For the invasion assay, the upper chamber was coated with 40  $\mu$ l BD Matrigel™ (BD Biosciences), which was initially dissolved in medium (1:8) and allowed to adhere to the chamber at 37°C for 4 h, and 600  $\mu$ l full medium containing 15% FBS was added to the lower chamber. After 48 h, uninvaded cells in the upper chamber were wiped off with cotton swabs, and invaded cells were fixed with 4% paraformaldehyde for 30 min at room temperature, and stained with 0.1% crystal violet for 30 min at room temperature. The number of invaded cells was counted under a light microscope (magnification, x200).

**Western blotting.** After 24 h of treatment with AA (10, 20 and 40  $\mu$ mol/l) with or without TGF- $\beta$ 1 (10 ng/ml), cells were washed twice with ice-cold PBS, centrifuged at 12,000 x g for 10 min at 4°C, lysed with radioimmunoprecipitation assay buffer (Beijing Solarbio Science & Technology Co., Ltd., Beijing, China) and incubated on ice for 20 min. The protein concentration was determined with a bicinchoninic acid protein assay kit (Thermo Fisher Scientific, Inc.). Total proteins (40  $\mu$ g) were separated by 10% SDS-PAGE and transferred onto a 0.45- $\mu$ m polyvinylidene fluoride membrane (EMD Millipore, Billerica, MA, USA). The membrane was blocked in a buffer containing 0.3 g bovine serum albumin (Sigma-Aldrich; Merck KGaA), 20 ml PBS with 20  $\mu$ l 0.1% Tween-20 (PBST; Beijing Solarbio Science & Technology Co., Ltd.) and 1 g non-fat milk at room temperature for 2 h. The membrane was then incubated with the primary antibodies against E-cadherin (1:1,000; cat. no. ab1416), N-cadherin (1:1,000; cat. no. ab18203),  $\beta$ -catenin (1:1,000; cat. no. ab16051), vimentin (1:1,000; cat. no. ab8978), snail family transcriptional repressor (Snail;

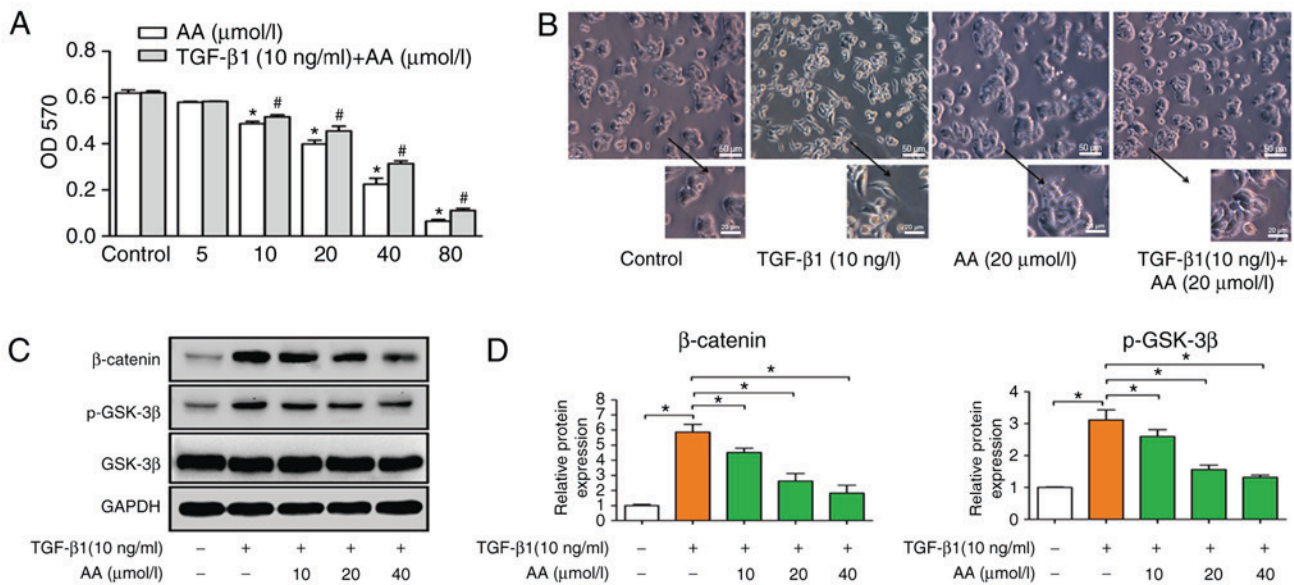


Figure 1. (A) Effects of AA on the viability of TGF- $\beta$ 1-treated A549 cells. \* $P < 0.05$ , compared with the AA control group; # $P < 0.05$ , compared with TGF- $\beta$ 1 + AA control group. (B) Morphological alterations of A549 cells (magnification,  $\times 400$ ) and (C) protein expression levels of  $\beta$ -catenin, p-GSK-3 $\beta$  and GSK-3 $\beta$  before and after TGF- $\beta$ 1 and AA treatment. (D) Semi-quantitative analysis of (C). \* $P < 0.05$ . AA, asiatic acid; GSK-3 $\beta$ , glycogen synthase kinase-3 $\beta$ ; OD, optical density; p-GSK-3 $\beta$ , phosphorylated-GSK-3 $\beta$ ; TGF- $\beta$ 1, transforming growth factor- $\beta$ 1.

1:1,000; cat. no. ab53519), glycogen synthase kinase-3 $\beta$  (GSK-3 $\beta$ ; 1:1,000; cat. no. ab93926) and GAPDH (1:2,000; cat. no. ab8245) all from Abcam, Cambridge, MA, USA, and phosphorylated-GSK-3 $\beta$  (p-GSK-3 $\beta$ ; 1:1,000; cat. no. CST #9336, Cell Signaling Technology, Inc., Danvers, MA, USA) overnight at 4°C. The membrane was then washed three times for 15 min with PBST, and incubated with a horseradish peroxidase (HRP)-conjugated secondary antibody (1:1,500; Abcam; cat. no. ab9482) for 2 h at room temperature. Enhanced chemiluminescence reagent (Bio-Rad Laboratories, Inc., Hercules, CA, USA) was used to detect the signal on the membrane. The data were analyzed via densitometry using the Gel Image Analysis system (Tanon 2500R, Shanghai, China) and normalized to the expression of the internal control (GAPDH).

**Reverse transcription-quantitative polymerase chain reaction (RT-qPCR).** Total RNA was isolated from A549 cells using TRIzol® reagent (Invitrogen; Thermo Fisher Scientific, Inc.) as previously described (22). cDNA was synthesized using a PrimeScript™ RT reagent kit (Takara Bio, Inc., Otsu, Japan) according to the manufacturer's protocol. cDNA was diluted 10 times and the SYBR-Green Supermix (Bio-Rad Laboratories, Inc.) was used to perform PCR using the Opticon 2 Real-time PCR Detection system (Bio-Rad Laboratories, Inc.). RT-qPCR reactions were performed as follows: Pre-denaturation at 95°C for 10 min, followed by 40 cycles of denaturation at 95°C for 10 sec, annealing at 58°C for 30 sec and extension at 72°C for 30 sec. The primers used for this experiment were designed as follows: Snail, forward, 5'-GAGGACAGTGGGAA GGCTC-3', reverse, 5'-TGGCTTCGGATGTGCATCTT-3'; E-cadherin, forward, 5'-GGGGTCTGTCTCATGGAAGTG-3', reverse, 5'-CAAATCCAAGCCCGTGGTG-3'; N-cadherin, forward, 5'-GGAAATGGAACTTGATGGCA-3', reverse, 5'-GGAGGGATGACCCAGTCTCT-3'; vimentin, forward, 5'-CTCTGGCACGTCTTGACCTT-3', reverse, 5'-TTGCGC

TCCTGAAAACTGC-3';  $\beta$ -catenin, forward, 5'-GTGACT CTCGGAGCGGGA-3', reverse, 5'-CAGGCAAACAGGTGC TCAAC-3'; GSK-3 $\beta$ , forward, 5'-GACTAAGGTCTTCCG ACCCC-3', reverse, 5'-TTAGCATCTGACGCTGCTGT-3'; and GAPDH, forward, 5'-AATGGGCAGCCGTTAGGA AA-3' and reverse, 5'-GCGCCCAATACGACCAAATC-3'. The relative mRNA expression levels were analyzed using the comparative cycle quantification (Cq) ( $2^{-\Delta\Delta Cq}$ ) method (23) and normalized to the endogenous control. Each sample was set up in triplicate and the experiments were repeated three times.

**Statistical analysis.** All experiments were performed three times and the data are expressed as the means  $\pm$  standard deviation. Unless stated otherwise, statistical analysis was performed using GraphPad Prism 5.01 software (GraphPad Software, Inc., La Jolla, CA, USA). Multiples comparisons were performed by one-way analysis of variance followed by Tukey's post hoc test.  $P < 0.05$  was considered to indicate a statistically significant difference.

## Results

**Effect of TGF- $\beta$ 1 on inhibition of A549 cells viability.** Cells were treated with increasing concentrations of AA (0, 5, 10, 20, 40 and 80  $\mu$ mol/l) with or without TGF- $\beta$ 1 (10 ng/ml) for 24 h. MTT assay was used to measure the effect of AA on A549 cell viability (Fig. 1A). Results demonstrated that AA significantly decreased cell viability in a dose-dependent manner; notably, a high concentration of AA inhibited the viability of A549 cells. Since the present study aimed to investigate whether a low concentration of AA could inhibit TGF- $\beta$ 1-induced EMT, the concentrations of AA used in subsequent experiments were 10, 20 and 40  $\mu$ mol/l. The viability of A549 cells treated with TGF- $\beta$ 1 (10 ng/ml) was not effected.



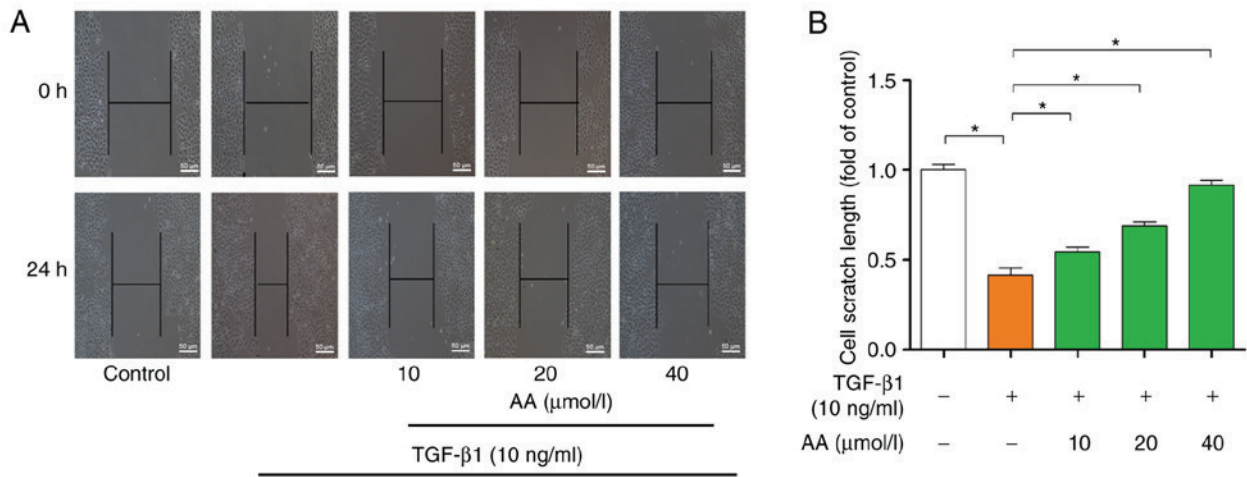


Figure 2. Migratory capacity of A549 cells following 24 h treatment with TGF- $\beta$ 1 with or without AA, as assessed by wound healing assay. (A) Representative image. (B) Quantitative analysis of (B). \*P<0.05. AA, asiatic acid; TGF- $\beta$ 1, transforming growth factor- $\beta$ 1.

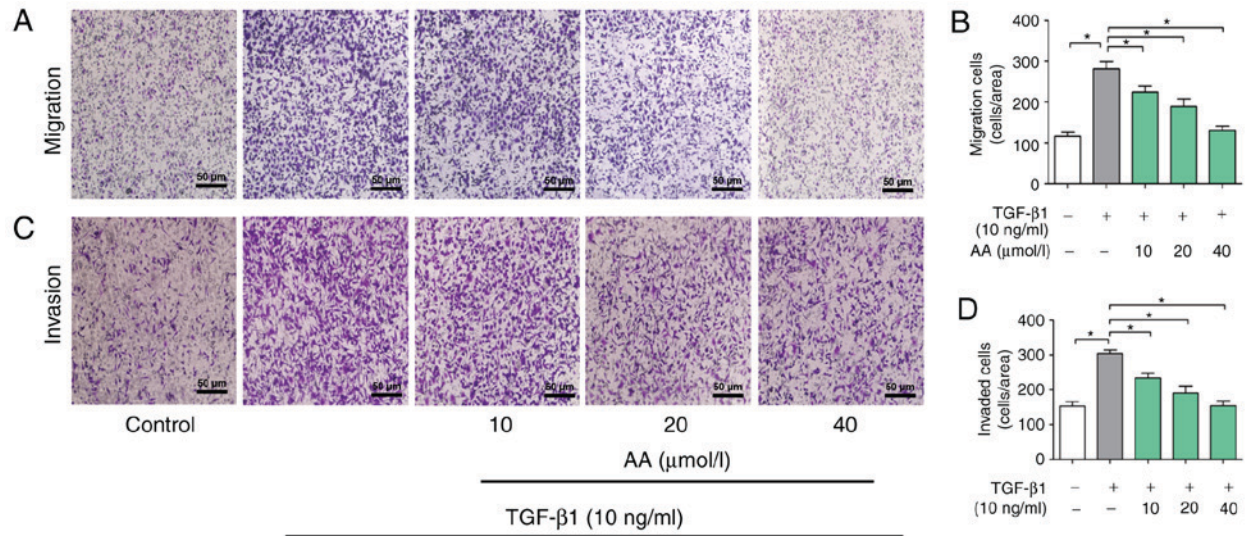


Figure 3. Effects of AA on the migration and invasion of TGF- $\beta$ 1-treated A549 cells. (A) Representative image of Transwell migration analysis of A549 cells treated with TGF- $\beta$ 1 and AA. (B) Quantitative analysis of (A). (C) Representative image of Transwell invasion analysis of A549 cells treated with TGF- $\beta$ 1 and AA. (D) Quantitative analysis of (C). \*P<0.05. AA, asiatic acid; TGF- $\beta$ 1, transforming growth factor- $\beta$ 1.

*TGF- $\beta$ 1 induces EMT of A549 cells.* A549 cells were treated with TGF- $\beta$ 1 (10 ng/ml) for 24 h to induce EMT. A549 cell morphology following TGF- $\beta$ 1 treatment was assessed under an inverted microscope. Results demonstrated that TGF- $\beta$ 1 induced a change in cell morphology, from the cobblestone to the fusiform shape, similar to fibroid cells. These results demonstrated that TGF- $\beta$ 1 allowed modification of the epithelial A549 cells into a mesenchymal phenotype. As presented in Fig. 1B, the control group exhibited an epithelial cell morphology with strong intercellular adhesion; however, following TGF- $\beta$ 1 treatment, cell morphology changed to fusiform, exhibiting the morphological characteristics of interstitial cells with few intercellular connections. Conversely, AA inhibited TGF- $\beta$ 1-induced EMT, as observed by cells that retained an epithelial morphology with few fusiform forms and increased intercellular adhesion, which confirmed that EMT was induced following 24 h treatment with TGF- $\beta$ 1 (Fig. 1B). In addition, AA treatment had no effect

on A549 cell morphology compared with the control group. Furthermore, western blotting demonstrated that  $\beta$ -catenin and p-GSK-3 $\beta$  protein expression levels were decreased by AA, while no difference in the expression level of GSK-3 $\beta$  was observed (Fig. 1C and D).

*Effect of AA on migration and invasion of TGF- $\beta$ 1-treated A549 cells.* The effects of AA on cell migration are presented in Fig. 2A. Compared with in the control group, 24 h TGF- $\beta$ 1 treatment significantly promoted A549 cell migration (P<0.05). However, AA treatment significantly (P<0.05) inhibited TGF- $\beta$ 1-induced A549 cell migration following 24 h of AA treatment. The effects of AA on scratch length are presented in Fig. 2B. Results indicated that AA significantly inhibited TGF- $\beta$ 1-induced A549 cell migration in a dose-dependent manner.

The role of AA on invasion of A549 cells was then determined. As presented in Fig. 3A and B, the migration of

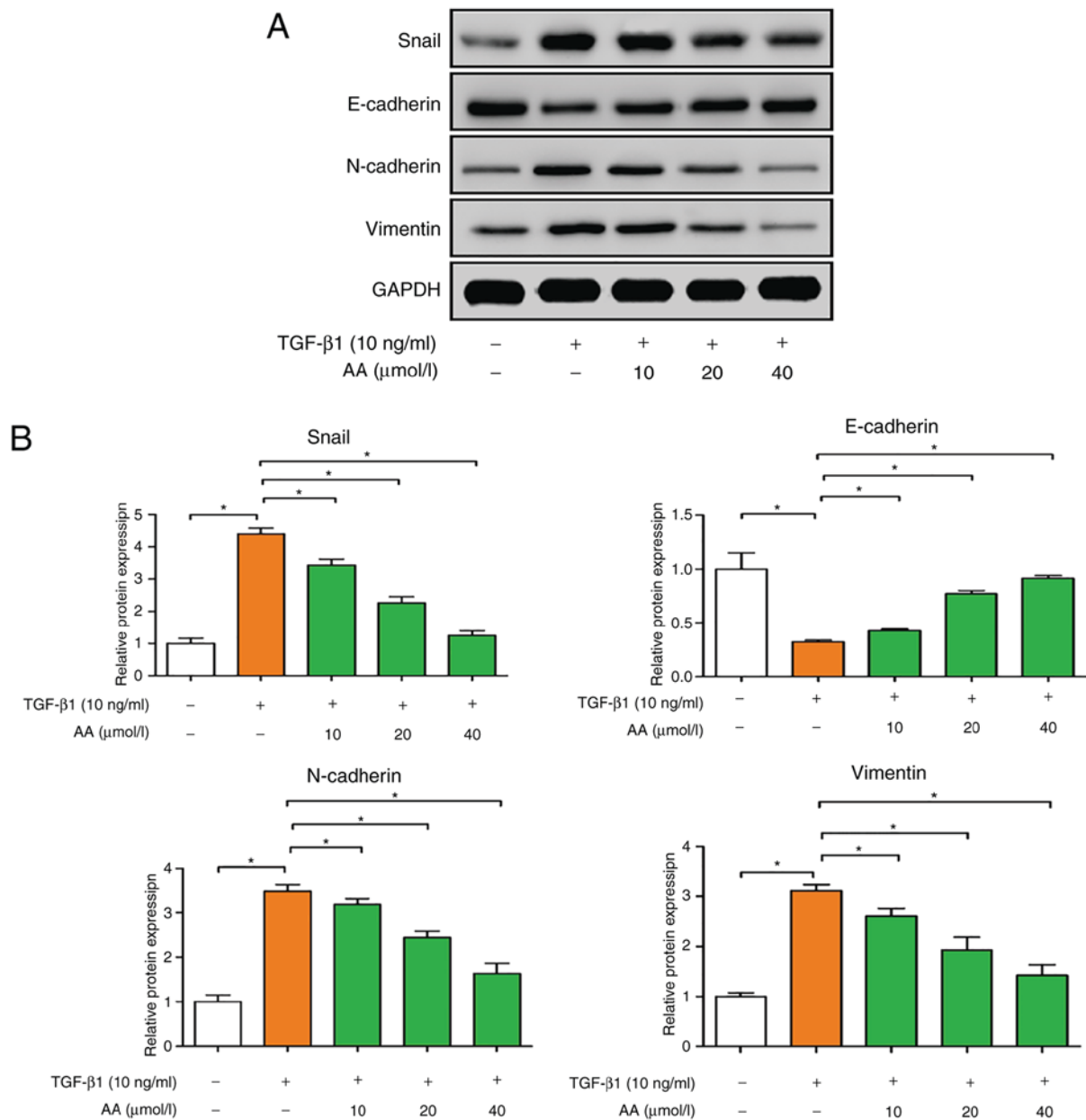


Figure 4. Effects of AA on Snail, E-cadherin, N-cadherin and vimentin protein expression in TGF-β1-treated A549 cells, as assessed by western blotting. (A) Representative images. (B) Semi-quantitative analysis of (A). \*P<0.05. AA, asiatic acid; Snail, snail family transcriptional repressor; TGF-β1, transforming growth factor-β1.

cells in the AA+ TGF-β1 treatment group was significantly inhibited compared with the cells in the TGF-β1 treatment group (P<0.05). Furthermore, TGF-β1 treatment significantly promoted A549 cell invasion in a dose-dependent manner (P<0.05). Conversely, 24 h treatment with AA significantly inhibited TGF-β1-induced cell invasion in a dose-dependent manner (P<0.05; Fig. 3C and D).

**AA regulates EMT-associated protein expression in A549 cells.** The effects of AA on the expression of EMT protein markers in A549 cells were examined by western blotting. As presented in Fig. 4A and B, TGF-β1-treated cells exhibited significantly decreased E-cadherin expression (P<0.05), and increased N-cadherin, vimentin and Snail expression (P<0.05), compared with the control group. Conversely, AA-treated

cells presented a significant increase in E-cadherin expression (P<0.05), and a significant decrease in N-cadherin, vimentin and Snail expression (P<0.05). These results suggested that AA may significantly inhibit EMT of A549 cells.

**AA regulates EMT-associated mRNA expression levels in A549 cells.** The effects of AA on EMT-associated mRNA expression levels in A549 cells were evaluated by RT-qPCR, as presented in Fig. 5. In TGF-β1-treated cells, E-cadherin expression levels were significantly decreased (P<0.05), whereas N-cadherin (P<0.05), Snail (P<0.05), vimentin and β-catenin expression levels were markedly increased compared with in the control group (P<0.05). However, combined cell treatment with TGF-β1 and AA significantly increased E-cadherin expression levels (P<0.05), but decreased the expression levels of

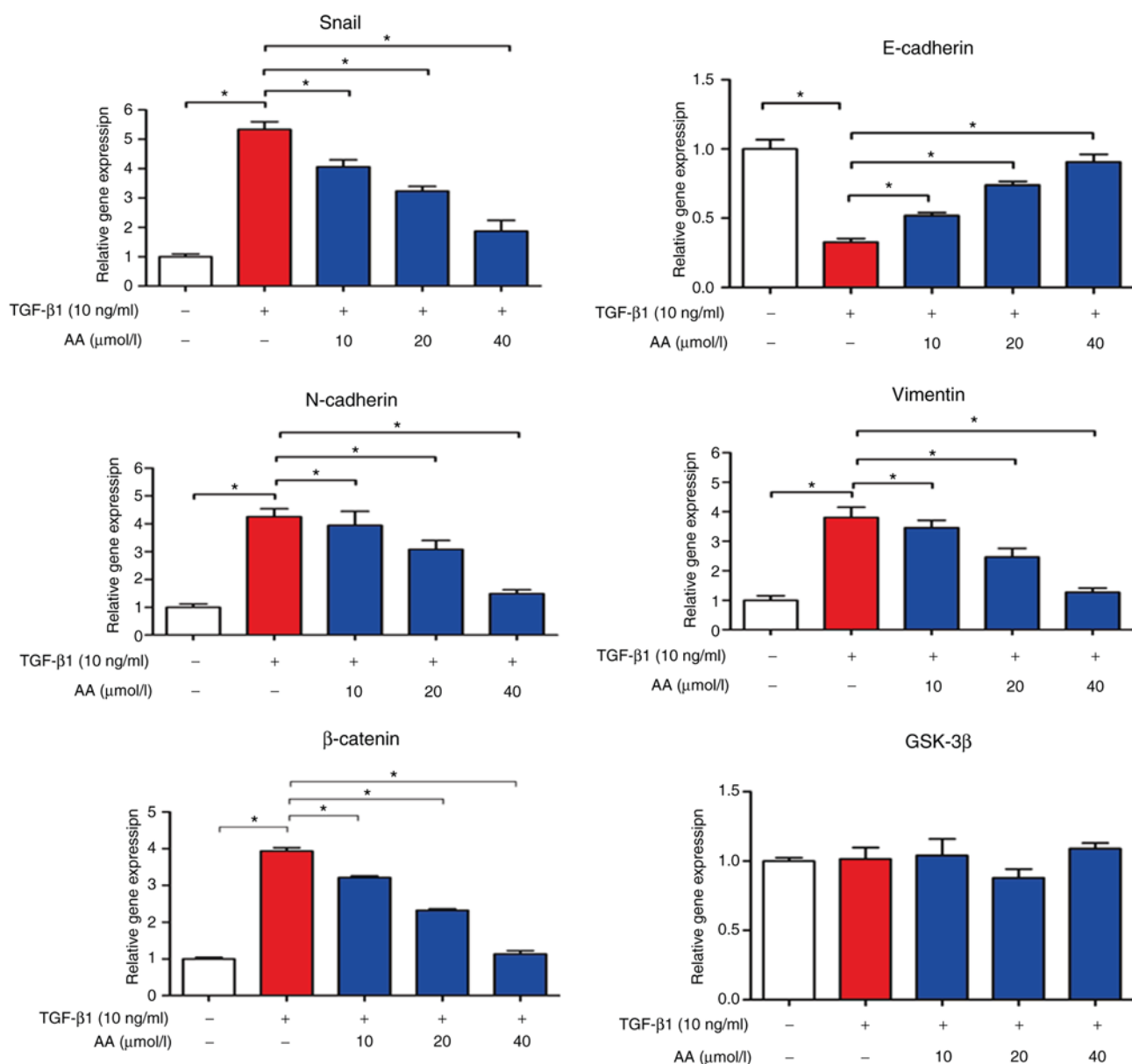


Figure 5. Effects of AA on Snail, E-cadherin, N-cadherin and vimentin expression levels in TGF- $\beta$ 1-treated A549 cells, as assessed by reverse transcription-quantitative polymerase chain reaction. \* $P < 0.05$ . AA, asitic acid; GSK-3 $\beta$ , glycogen synthase kinase-3 $\beta$ ; Snail, snail family transcriptional repressor; TGF- $\beta$ 1, transforming growth factor- $\beta$ 1.

N-cadherin, vimentin, Snail and  $\beta$ -catenin compared with in TGF- $\beta$ 1-treated cells ( $P < 0.05$ ). No change in GSK-3 $\beta$  expression level was observed in A549 cells treated with TGF- $\beta$ 1 with or without AA. These results suggested that AA may significantly inhibit EMT of A549 cells.

## Discussion

Lung cancer is one of the most common types of cancer worldwide and is one of the leading causes of cancer-associated mortality. In China, the increasing incidence of lung cancer and lung-cancer-associated mortality have become serious health issues. At present, the 5-year survival rate remains poor (~18%), since >57% of lung cancer cases are diagnosed at a distant stage (2). Understanding the biological characteristics of lung cancer and the molecular mechanism underlying invasion and metastasis is therefore crucial. Metastasis is the main

biological process that distinguishes benign from malignant tumors, and is an underlying cause of mortality in patients with malignant tumors; however, the mechanism of tumor metastasis is very complex and remains incompletely understood. EMT has been reported as an important biological process of epithelial cell-derived tumor cells that undergo migration and invasion (24,25).

EMT involves the transformation of epithelial cells into interstitial cells and serves crucial roles in embryonic development, chronic inflammation, tissue reconstruction and cancer metastasis (26). EMT is associated with decreased expression of the cell adhesion molecule E-cadherin, increased expression of the cytoskeletal component vimentin and by enhanced characteristic morphology of mesenchymal cells (27-29). TGF- $\beta$ 1 is an EMT-inducible factor that activates the TGF- $\beta$ 1 signaling pathway in epithelial cells and promotes EMT occurrence, reduces tumor cell adhesion and

enhances invasion in certain types of cancer, including breast, lung, liver, colon and pancreatic cancer (30-32).  $\beta$ -catenin is the main structural component of intercellular adhesion, and abnormal alterations in its expression are associated with tumor infiltration and metastasis (33). The protein p-GSK-3 $\beta$  is a multifunctional serine threonine kinase, which regulates the activation of various signaling pathways and serves important roles in protein expression, and tumor cell proliferation and apoptosis. GSK-3 $\beta$  is considered to be the major negative regulatory factor for  $\beta$ -catenin, and its inactivation can cause cell cycle disturbance and accelerate tumor proliferation (34). In the present study, an EMT model of lung cancer was established through the treatment of A549 cells with TGF- $\beta$ 1. Following 24 h TGF- $\beta$ 1 treatment, A549 cells became fusiform and presented interstitial cell features. In addition, the treatment of A549 cells with TGF- $\beta$ 1 increased  $\beta$ -catenin and p-GSK-3 $\beta$  protein expression levels. These results were consistent with previous studies, which suggested that TGF- $\beta$ 1 may induce EMT transformation of lung cancer cells (35,36).

EMT is a dynamic multi-step process that occurs prior to tumor cell metastasis. These cells acquire the migratory and invasive abilities of mesenchymal cells, which allow their entry into the bloodstream and lymph channels for distant metastasis (37). In the present study, AA significantly inhibited invasion and migration of TGF- $\beta$ 1-treated cells, which suggested that AA may prevent cell metastasis by inhibiting EMT of A549 cells.

E-cadherin and N-cadherin belong to the cadherin family; the extracellular domains of cadherin proteins share immunoglobulin-like structure with the N-terminal domain. E-cadherin forms an E-cadherin/ $\beta$ -catenin complex through connection of  $\beta$ -catenin and cytoskeleton protein (38,39). The E-cadherin/ $\beta$ -catenin complex interferes with cell adhesion, and inhibits tumor cell invasion and metastasis (30). N-cadherin induces EMT by affecting E-cadherin-associated cell adhesion, which gives cancer cells an invasive and malignant phenotype (40). Vimentin is an important cytoskeletal protein that is mainly present in mesenchymal tissues and cells. A previous study reported that vimentin is closely associated with tumor metastasis (41). Furthermore, Snail is a transcriptional regulator and an upstream regulator of E-cadherin, which negatively regulates E-cadherin expression. When EMT occurs, Snail is upregulated and E-cadherin is downregulated, which promotes the transition of epithelial cells to a mesenchymal phenotype to promote tumor metastasis (42). In the present study, AA markedly upregulated E-cadherin mRNA and protein expression levels; however, Snail, N-cadherin, vimentin and  $\beta$ -catenin expression levels were downregulated by AA in TGF- $\beta$ 1-treated cells. These results suggested that AA may inhibit EMT of A549 cells.

In conclusion, the present study suggested that AA may inhibit migration and invasion of A549 cells through EMT inhibition. This finding provided novel foundations for the treatment of lung cancer, and supplied theoretical and experimental evidence for the use of AA as an EMT inhibitor.

#### Acknowledgements

Not applicable.

#### Funding

This study was supported by The Traditional Chinese Medicine in Henan Province (grant no. 2017ZY2063).

#### Availability of data and materials

The datasets used and analyzed during the current study are available from the corresponding author on reasonable request.

#### Authors' contributions

QC and QZ designed the experiments. QC, JR, QY and BL performed the experiments. QC, JR, QY and BL analyzed the data. QC and JR wrote the manuscript. QC and JR revised the manuscript. All authors read and approved the final manuscript.

#### Ethics approval and consent to participate

Not applicable.

#### Patients consent for publication

Not applicable.

#### Competing interests

The authors declare that they have no competing interests.

#### References

- Feng B, Zhang K, Wang R and Chen L: Non-small-cell lung cancer and miRNAs: Novel biomarkers and promising tools for treatment. *Clin Sci (Lond)* 128: 619-634, 2015.
- Siegel RL, Miller KD and Jemal A: Cancer statistics, 2018. *CA Cancer J Clin* 68: 7-30, 2018.
- World Health Organization; 2002. [https://www.who.int/bulletin/archives/80\(1\)78.pdf](https://www.who.int/bulletin/archives/80(1)78.pdf). Accessed June 18, 2018.
- Smith CB, Kelley AS and Meier DE: Evidence for new standard of care in non-small cell lung cancer patients. *Semin Thorac Cardiovasc Surg* 22: 193-194, 2010.
- Stuschke M, Eberhardt W, Pöttgen C, Stamatis G, Wilke H, Stüben G, Stöblen F, Wilhelm HH, Menker H, Teschler H, *et al*: Prophylactic cranial irradiation in locally advanced non-small-cell lung cancer after multimodality treatment: Long-term follow-up and investigations of late neuropsychologic effects. *J Clin Oncol* 17: 2700-2709, 1999.
- Minguet J, Smith KH and Bramlage P: Targeted therapies for treatment of non-small cell lung cancer-recent advances and future perspectives. *Int J Cancer* 138: 2549-2561, 2015.
- Xu JH, Yang HP, Zhou XD, Wang HJ, Liang G and Tang CL: Role of Wnt inhibitory factor-1 in inhibition of bisdemethoxycurcumin mediated epithelial-to-mesenchymal transition in highly metastatic lung cancer 95D cells. *Chin Med J (Engl)* 128: 1376-1383, 2015.
- Wu T, Geng J, Guo W, Gao J and Zhu X: Asiatic acid inhibits lung cancer cell growth in vitro and in vivo by destroying mitochondria. *Acta Pharm Sin B* 7: 65-72, 2017.
- Lu Y, Liu S, Wang Y, Wang D, Gao J and Zhu L: Asiatic acid uncouples respiration in isolated mouse liver mitochondria and induces HepG2 cells death. *Eur J Pharmacol* 786: 212-223, 2016.
- Ren L, Cao QX, Zhai FR, Yang SQ and Zhang HX: Asiatic acid exerts anticancer potential in human ovarian cancer cells via suppression of PI3K/Akt/mTOR signalling. *Pharm Biol* 54: 2377-2382, 2016.
- Park BC, Paek SH, Lee YS, Kim SJ, Lee ES, Choi HG, Yong CS and Kim JA: Inhibitory effects of asiatic acid on 7,12-dimethylbenz[a]anthracene and 12-O-tetradecanoylphorbol 13-acetate-induced tumor promotion in mice. *Biol Pharm Bull* 30: 176-179, 2007.



12. Tang XL, Yang XY, Jung HJ, Kim SY, Jung SY, Choi DY, Park WC and Park H: Asiatic acid induces colon cancer cell growth inhibition and apoptosis through mitochondrial death cascade. *Biol Pharm Bull* 32: 1399-1405, 2009.
13. Yilmaz M and Christofori G: EMT, the cytoskeleton, and cancer cell invasion. *Cancer Metastasis Rev* 28: 15-33, 2009.
14. Ke Y, Zhao W, Xiong J and Cao R: miR-149 inhibits non-small-cell lung cancer cells EMT by targeting FOXM1. *Biochem Res Int* 2013: 506731, 2013.
15. Roy BC, Kohno T, Iwakawa R, Moriguchi T, Kiyono T, Morishita K, Sanchez-Cespedes M, Akiyama T and Yokota J: Involvement of LKB1 in epithelial-mesenchymal transition (EMT) of human lung cancer cells. *Lung Cancer* 70: 136-145, 2010.
16. Shen SJ, Zhang YH, Gu XX, Jiang SJ and Xu LJ: Yangfei Kongliu formula, a compound Chinese herbal medicine, combined with cisplatin, inhibits growth of lung cancer cells through transforming growth factor- $\beta$ 1 signaling pathway. *J Integr Med* 15: 242-251, 2017.
17. Al-Saad S, Al-Shibli K, Donnem T, Persson M, Bremnes RM and Busund LT: The prognostic impact of NF- $\kappa$ B p105, vimentin, E-cadherin and Par6 expression in epithelial and stromal compartment in non-small-cell lung cancer. *Br J Cancer* 99: 1476-1483, 2008.
18. Zhang HJ, Wang HY, Zhang HT, Su JM, Zhu J, Wang HB, Zhou WY, Zhang H, Zhao MC, Zhang L and Chen XF: Transforming growth factor- $\beta$ 1 promotes lung adenocarcinoma invasion and metastasis by epithelial-to-mesenchymal transition. *Mol Cell Biochem* 355: 309-314, 2011.
19. Zang QQ, Lu Z, Ning G and Cheng H: Ophiopogonin D inhibits cell proliferation, causes cell cycle arrest at G2/M, and induces apoptosis in human breast carcinoma MCF-7 cells. *J Integr Med* 14: 51-59, 2016.
20. Liu JJ, Liu JY, Chen J, Wu YX, Yan P, Ji CD, Wang YX, Xiang DF, Zhang X, Zhang P, *et al*: Scinderin promotes the invasion and metastasis of gastric cancer cells and predicts the outcome of patients. *Cancer Lett* 376: 110-117, 2016.
21. Uygun K, Bilici A, Kaya S, Oven Ustaalioglu BB, Yildiz R, Temiz S, Seker M, Aksu G, Cabuk D and Gumus M: XELIRI plus bevacizumab compared with FOLFIRI plus bevacizumab as first-line setting in patients with metastatic colorectal cancer: Experiences at two-institutions. *Asian Pac J Cancer Prev* 14: 2283-2288, 2013.
22. Beekman JM, Reischl J, Henderson D, Bauer D, Ternes R, Peña C, Lathia C and Heubach JF: Recovery of microarray-quality RNA from frozen EDTA blood samples. *J Pharmacol Toxicol Methods* 59: 44-49, 2009.
23. Livak KJ and Schmittgen TD: Analysis of relative gene expression data using real-time quantitative PCR and the 2<sup>-</sup>(Delta Delta C(T)) method. *Methods* 25: 402-408, 2001.
24. Yang J and Weinberg RA: Epithelial-mesenchymal transition: At the crossroads of development and tumor metastasis. *Dev Cell* 14: 818-829, 2008.
25. Nagathihalli NS, Massion PP, Gonzalez AL, Lu P and Datta PK: Smoking induces epithelial-to-mesenchymal transition in Non-small cell lung cancer through HDAC-mediated downregulation of E-cadherin. *Mol Cancer Ther* 11: 2362-2372, 2012.
26. Aref AR, Huang RYJ, Kang W, Jing SW, Thiery JP and Kamm RD: Transitions between epithelial and mesenchymal states in microfluidic platform: Acquisition of malignant and stem cell traits, 2013.
27. Kiesslich T, Pichler M and Neureiter D: Epigenetic control of epithelial-mesenchymal-transition in human cancer. *Mol Clin Oncol* 1: 3-11, 2013.
28. Zhao R, Gong L, Li L, Guo L, Zhu D, Wu Z and Zhou Q: nM23-H1 is a negative regulator of TGF- $\beta$ 1-dependent induction of epithelial-mesenchymal transition. *Exp Cell Res* 319: 740-749, 2013.
29. Reinhold WC, Reimers MA, Lorenzi P, Ho J, Shankavaram UT, Ziegler MS, Bussey KJ, Nishizuka S, Ikediobi O, Pommier YG and Weinstein JN: Multifactorial regulation of E-cadherin expression: An integrative study. *Mol Cancer Ther* 9: 1-16, 2010.
30. Cho KH, Yu SL, Cho DY, Chang GP and Hoi YL: Breast cancer metastasis suppressor 1 (BRMS1) attenuates TGF- $\beta$ 1-induced breast cancer cell aggressiveness through downregulating HIF-1 $\alpha$  expression. *BMC Cancer* 15: 829, 2015.
31. Toba-Ichihashi Y, Yamaoka T, Ohmori T and Ohba M: Up-regulation of Syndecan-4 contributes to TGF- $\beta$ 1-induced epithelial to mesenchymal transition in lung adenocarcinoma A549 cells. *Biochem Biophys Rep* 5: 1-7, 2015.
32. Li Y, Zhu G, Zhai H, Jia J, Yang W, Li X and Liu L: Simultaneous stimulation with tumor necrosis factor- $\alpha$  and transforming growth factor- $\beta$ 1 induces epithelial-mesenchymal transition in colon cancer cells via the NF- $\kappa$ B pathway. *Oncol Lett* 15: 6873-6880, 2018.
33. Ding Y, Shen S, Lino AC, Curotto de Lafaille MA and Lafaille JJ: Beta-catenin stabilization extends regulatory T cell survival and induces anergy in nonregulatory T cells. *Nat Med* 14: 162-169, 2008.
34. Shakoori A, Ougolkov A, Yu ZW, Zhang B, Modarressi MH, Billadeau DD, Mai M, Takahashi Y and Minamoto T: Deregulated GSK3 $\beta$  activity in colorectal cancer: Its association with tumor cell survival and proliferation. *Biochem Biophys Res Commun* 334: 1365-1373, 2005.
35. Singh A and Settleman J: EMT, cancer stem cells and drug resistance: An emerging axis of evil in the war on cancer. *Oncogene* 29: 4741-4751, 2010.
36. Lin XL, Liu M, Liu Y, Hu H, Pan Y, Zou W, Fan X and Hu X: Transforming growth factor  $\beta$ 1 promotes migration and invasion in HepG2 cells: Epithelial-to-mesenchymal transition via JAK/STAT3 signaling. *Int J Mol Med* 41: 129-136, 2018.
37. Talmadge JE and Fidler IJ: AACR centennial series: The biology of cancer metastasis: Historical perspective. *Cancer Res* 70: 5649-5669, 2010.
38. Macdonald PR, Progius P, Ciani B, Patel S, Mayer U, Steinmetz MO and Kammerer RA: Structure of the extracellular domain of Tie receptor tyrosine kinases and localization of the angiopoietin-binding epitope. *J Biol Chem* 281: 28408-28414, 2006.
39. Abuetabh Y, Persad S, Nagamori S, Huggins J, Al-Bahrani R and Sergi C: Expression of E-cadherin and  $\beta$ -catenin in two cholangiocarcinoma cell lines (OZ and HuCCT1) with different degree of invasiveness of the primary tumor. *Ann Clin Lab Sci* 41: 217-223, 2011.
40. Chunhacha P, Sriuranpong V and Chanvorachote P: Epithelial-mesenchymal transition mediates anoikis resistance and enhances invasion in pleural effusion-derived human lung cancer cells. *Oncol Lett* 5: 1043-1047, 2013.
41. Zhang H, Liu J, Yue D, Gao L, Wang D, Zhang H and Wang C: Clinical significance of E-cadherin,  $\beta$ -catenin, vimentin and S100A4 expression in completely resected squamous cell lung carcinoma. *J Clin Pathol* 66: 937-945, 2013.
42. Battle E, Sancho E, Francí C, Domínguez D, Monfar M, Baulida J and García De Herreros A: The transcription factor snail is a repressor of E-cadherin gene expression in epithelial tumour cells. *Nat Cell Biol* 2: 84-89, 2000.



This work is licensed under a Creative Commons Attribution-NonCommercial-NoDerivatives 4.0 International (CC BY-NC-ND 4.0) License.